An MRI-compatible system for focused ultrasound experiments in small animal models

Rajiv Chopra[a)]
Imaging Research, Sunnybrook Health Sciences Centre, 2075 Bayview Avenue, Toronto, Ontario M4N 3M5, Canada and Department of Medical Biophysics, University of Toronto, 610 University Avenue, Toronto, Ontario M5G 2M9, Canada

Laura Curiel
Imaging Research, Sunnybrook Health Sciences Centre, 2075 Bayview Avenue, Toronto, Ontario M4N 3M5, Canada and HIFU Laboratory, Thunder Bay Regional Research Institute, 980 Oliver Road, Thunder Bay, Ontario P7B 6V4, Canada

Robert Staruch
Imaging Research, Sunnybrook Health Sciences Centre, 2075 Bayview Avenue, Toronto, Ontario M4N 3M5, Canada and Department of Medical Biophysics, University of Toronto, 610 University Avenue, Toronto, Ontario M5G 2M9, Canada

Laetitia Morrison
Imaging Research, Sunnybrook Health Sciences Centre, 2075 Bayview Avenue, Toronto, Ontario M4N 3M5, Canada

Kullervo Hynynen
Imaging Research, Sunnybrook Health Sciences Centre, 2075 Bayview Avenue, Toronto, Ontario M4N 3M5, Canada and Department of Medical Biophysics, University of Toronto, 610 University Avenue, Toronto, Ontario M5G 2M9, Canada

(Received 25 November 2008; revised 25 February 2009; accepted for publication 17 March 2009; published 24 April 2009)

The development of novel MRI-guided therapeutic ultrasound methods including potentiated drug delivery and targeted thermal ablation requires extensive testing in small animals such as rats and mice due to the widespread use of these species as models of disease. An MRI-compatible, computer-controlled three-axis positioning system was constructed to deliver focused ultrasound exposures precisely to a target anatomy in small animals for high-throughput preclinical drug delivery studies. Each axis was constructed from custom-made nonmagnetic linear ball stages driven by piezoelectric actuators and optical encoders. A range of motion of $5\times5\times2.5$ cm^3 was achieved, and initial bench top characterization demonstrated the ability to deliver ultrasound to the brain with a spatial accuracy of 0.3 mm. Operation of the positioning system within the bore of a clinical 3 T MR imager was feasible, and simultaneous motion and MR imaging did not result in any mutual interference. The system was evaluated in its ability to deliver precise sonications within the mouse brain, linear scanned exposures in a rat brain for blood barrier disruption, and circular scans for controlled heating under MR temperature feedback. Initial results suggest that this is a robust and precise apparatus for use in the investigation of novel ultrasound-based therapeutic strategies in small animal preclinical models. [DOI: 10.1118/1.3115680]

Key words: MRI-guided focused ultrasound, positioning, preclinical, MRI compatible

I. INTRODUCTION

MRI-guided focused ultrasound therapy is gaining use as a noninvasive method for thermal tissue coagulation[1–3] with significant promise as a tool to potentiate biologic therapies,[4,5] achieve focal disruption of the blood-brain barrier (BBB), and generate targeted heating of tissue for drug delivery and activation.[6–8] Unlike tissue coagulation, however, the underlying mechanisms and optimal strategies for using ultrasound to potentiate therapies are still under investigation. The widespread translation of this technology into clinical practice still requires extensive testing in preclinical models of human disease. Small animals such as rats and mice are used frequently in biomedical research as models of human disease, and the small size of these animals makes focused ultrasound experiments difficult. Often, the ultrasound beam focal volume is comparable to the size of the target organs in these animals, requiring precise localization of energy in order to avoid exposure (and consequent damage) to surrounding structures.

Another challenge for the development of novel focused ultrasound applications such as drug delivery across the blood-brain barrier is the multitude of acoustic parameters that influence the desired biologic effect. These include frequency, pressure amplitude, exposure time, pulse duration, and pulse repetition frequency.[9] In addition, the type, concentration, and timing of the administered ultrasound con-

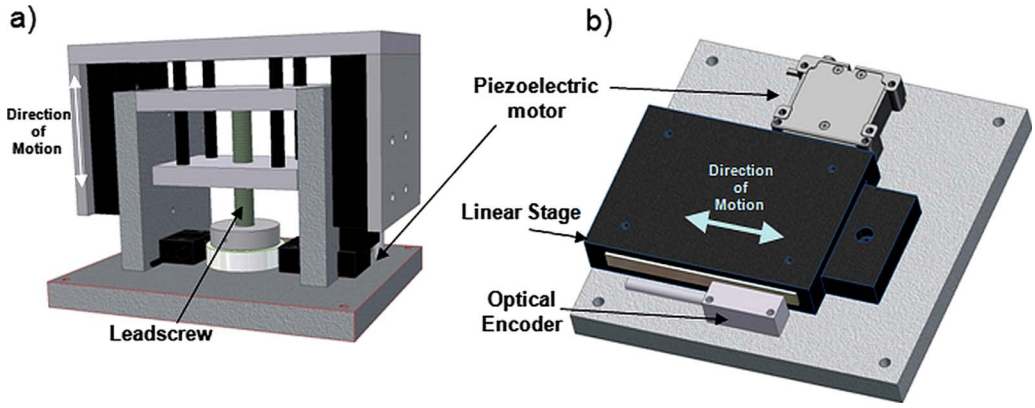

FIG. 1. Schematic of the MRI-compatible focused ultrasound system for small animals. The maximum travel in the horizontal planes (x,y) is 5 cm, and the travel in the vertical plane (z) is 2.5 cm. The spatial precision achievable with this system is approximately 0.05 mm.

trast agent are important parameters determining the biological effect in the brain.[9–12] The optimal exposure parameters may vary for different therapeutic agents depending on their size and properties.[13] Given this multidimensional problem, a large number of experimental investigations in small animal models may be required in order to elucidate both the mechanisms and optimal delivery strategies for a particular therapy. Focused ultrasound systems capable of delivering precise exposures to the brains (or other organs) of small animal models are an important tool for executing the studies required to determine safe and effective operating parameters for the clinical translation of novel therapeutic methods.

Performing focused ultrasound experiments in an MR imager offers a number of advantages including the ability to visualize anatomical targets in three dimensions and to monitor and evaluate the therapeutic effects *in vivo*. Furthermore, the temporal evolution of the response to therapy can be evaluated since animals can be imaged repeatedly in longitudinal studies. Experiments in the MR environment can be challenging, however, due to the difficulty in developing experimental systems that are compatible with the strong magnetic fields present. Most of the studies performed in rodent models with focused ultrasound in the MR environment have been performed with manual positioning systems[13–15] which, in addition to being slow, limit the types of experiments possible to simple exposures of a few points in the brain. An MRI-compatible focused ultrasound system capable of automatically targeting and exposing arbitrary regions in the brain in rodent models would be an important platform technology in the development of this field.

MRI-compatible positioning systems have been built previously for a variety of applications including surgical robotics,[16–18] biopsy procedures,[19–21] and focused ultrasound experiments in both humans and animals.[3,22–26] Positioning has been accomplished through the use of pneumatics, piezoceramic motors, and hydraulic systems due to the inability to use traditional motors in an MR imager. None of these systems have been specifically designed or characterized for delivering focused ultrasound exposures in small animals such as rats and mice for studies in targeted drug delivery to the brain. The purpose of this study was to develop a compact MRI-compatible system for focused ultrasound therapy in small animal models and to evaluate its performance in a closed-bore 3.0 T MR imager. A prototype system has been used for over a year in ongoing focused ultrasound experiments, and examples of the types of experiments achievable with this technology are presented in order to demonstrate the capabilities of this experimental platform for preclinical MRI-guided focused ultrasound research.

II. MATERIALS AND METHODS

II.A. Positioning system

Accurate exposure of anatomical targets requires the capability to position the focal zone at a desired position. To accomplish this, a three-axis motorized positioning system was built using non-magnetic components. Linear motion was achieved using piezoceramic actuators (HR4, Nanomotion Ltd., Yokneam, Israel) and optical encoders (LIA20, Numerik Jena, Jena, Germany). Precision motion was achieved by mounting the actuators onto a custom-made linear ball slide for each axis. The ball slides were constructed of aluminum for the carriage and slide, with beryllium copper races and ceramic balls. The linear ball slide design was effective for horizontal motion but not suitable for vertical motion caused by the unbalanced load on the stage due to the gravitational forces. In order to achieve a more robust vertical motion, a brass lead-screw driven ball slide was developed, with two piezoelectric actuators (HR2, Nanomotion Ltd., Israel) rotating a ceramic ring attached to the lead screw. 3D models of the horizontal and vertical axes are shown in Fig. 1. The horizontal stages were capable of moving up to 10 kg reliably. A single linear axis was used to perform simultaneous MR and ultrasound imaging in a previous study.[27]

An aluminum arm extending from the positioning system was used to hold a focused ultrasound transducer for experiments. The transducer was located in a water tank with an opening at the top for the placement of animals to be exposed to ultrasound energy. Embedded into the surface of the tank at the acoustic window was a custom-made single-loop rf receive coil used to acquire high-resolution MR images in

the vicinity of the exposed region of the tissue. The shape of the rf coil was rectangular, and a hole was cut out in the center to enable transmission of ultrasound. The size of the rf coil was chosen to fit snugly around the skull of the animal (rat/mouse) involved in the experiment. The tank was filled with degassed water during experiments to ensure good acoustic coupling of the animal to the transducer. All electrical cables powering the motors and encoders were passed into the magnet room through filtered low-pass connectors on a grounded rf-penetration panel. The motion of the system was achieved using a PCI-based servo controller (PCI-7344, National Instruments, Austin, TX) under C++ control.

II.B. Generation of the ultrasound beam

The system used to generate the ultrasound energy in all the experiments was comprised of a function generator (model 395, Wavetek, San Francisco, CA), RF amplifier (240L, ENI, West Henrietta, NY), and custom-made passive *L-C* matching circuit. All of the electronics were located outside the magnet room, except for the passive matching circuit which was placed at the end of the patient table of the MRI. The placement of the circuit at this location was due to the presence of a ferromagnetic toroid used in the inductor. The forward and reflected power was measured during power delivery using a dual-directional coupler (C2625, Werlatone, Brewster, NY) and an RF power meter (438A, Hewlett-Packard, Santa Clara, CA). For multi-point linear or circular trajectories, the motion controller located on the control PC produced a TTL signal upon reaching each position that was used to trigger the function generator to either produce a burst signal or to adjust the amplitude of the signal. The RF signal to the ultrasound transducer was passed through a grounded RF-penetration panel in the magnet room to eliminate any interference.

II.C. Accuracy measurements

Range of motion and accuracy of spatial positioning were measured for the prototype system both on the bench top and in a closed-bore 3.0 T MR imager (Signa, GE Healthcare, USA). Accuracy was evaluated by performing fixed motion paths and comparing measured with desired positions. The motion paths ranged from fast linear raster scans (i.e., six positions per second separated by 1 mm) to circular scans of different radii. The accuracy with which the system returned to its home position was also evaluated since this might be performed multiple times during a typical experiment. Initial tests in the MRI revealed that vibration of the patient table during imaging transmitted to the positioning system and caused undesirable drift in some of the axes of the positioner. This was resolved by keeping the servomotors active during imaging to counter these forces and maintain the stages fixed in place.

The spatial accuracy of focused ultrasound delivery using this system was evaluated initially in a series of gel experiments. An absorbing gel phantom made from 15% gelatin (Sigma-Aldrich, St. Louis, MO) was placed over the opening and a series of target locations in the gel were chosen based on MR images. The gelatin phantom was chosen for simplicity but is not necessarily an optimal absorber of ultrasound energy. Subsequently, the positioning system moved the transducer to each location and a continuous wave exposure of ultrasound was delivered at the acoustic power of approximately 10 W with the intention of generating a localized temperature elevation in the phantom. Gradient echo images (FSPGR, TE=2.2 ms, TR=76 ms, 128×128, slice=3 mm, FOV=12 cm, FA=30°) were acquired in rapid succession (every 10 s) transverse to the ultrasound beam to visualize the temperature changes in the gel manifested as a signal loss in the magnitude images due to changes in T_1. The accuracy of the focal positioning was evaluated by measuring the distance (in MR coordinates) between the desired target position and the measured location of heating.

II.D. Registration of MRI and positioner coordinates

All experiments described in this paper were performed on a clinical 3 T closed-bore MR imager (GE Signa, GE Healthcare, USA). For all experiments, an initial calibration between the coordinate space of the positioning system and the MRI is performed by heating an absorbing gel (Kitecko; 3M, St. Paull, MN) placed in the beam path. The gel is sonicated continuously at high power (15–20 W) to generate localized temperature elevation. Successive gradient echo images (FSPGR, TE=2.2 ms, TR=76 ms, 128×128, slice =3 mm, FOV=12 cm, FA=30°) are acquired transverse to the ultrasound beam at the focal location which depicts the heating as a localized region of reduced signal intensity. The focal location in depth is known based on the focal length of the transducer (measured using a hydrophone tank), as well as measurements of the heating pattern made with MR thermometry. The MRI coordinates of this localized heating are measured and related to the positioning system coordinates. This initial coordinate calibration enables all subsequent positioning to be prescribed and measured in the coordinates of the MRI.

II.E. Single location sonications in the brain

A series of sonications was performed in the brains of Swiss Webster mice (n=6), weighing 30–40 g. These exposures were performed to evaluate the capability to disrupt the blood-brain barrier in the same brain location in multiple animals. Two target regions within the midbrain (one in each hemisphere, spaced 4 mm apart) were chosen, and focused ultrasound exposures intended to disrupt the blood-brain barrier[28,29] were delivered. The ultrasound exposures were delivered in 10 ms bursts at 1.08 MHz, with a repetition frequency of 1 Hz. Immediately prior to sonication, a bolus injection of ultrasound contrast agent (0.02 ml/kg, Definity, Bristol Myers-Squibb, New York, NY) was administered through the tail vein of the animals with a flush of saline (0.1–0.2 ml). The duration of the sonications was 5 min, and the electrical power delivered to the transducer ranged from 0.25 to 1.0 W. The variation in power was not necessary for this study and was performed as part of another parametric study. The transducer used for these exposures was spheri-

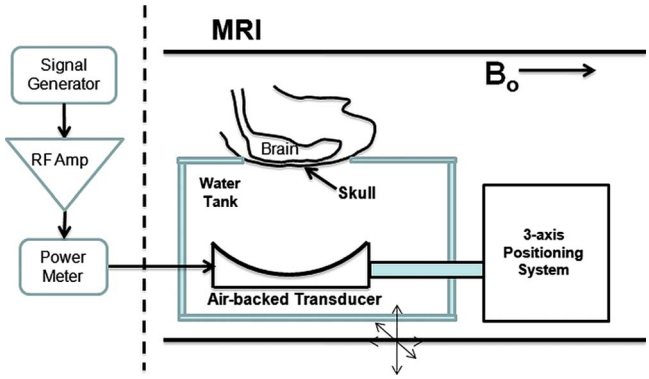

FIG. 2. General experimental setup for all the experiments using the focused ultrasound system. The difference between experiments was the positioning of the animal over the transducer and the ultrasound exposure performed in the body.

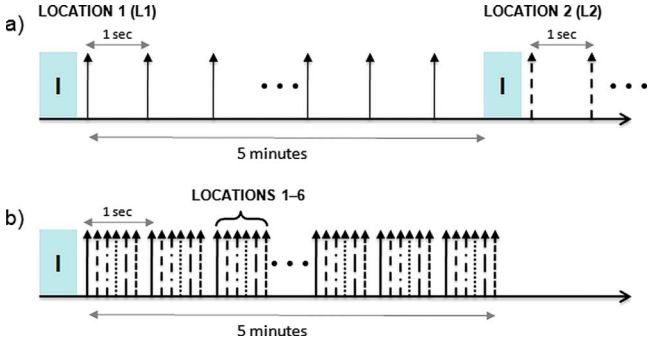

FIG. 3. Increased throughput of BBB experiments can be achieved by using a multiple spot sonication approach with the positioning system. A conventional approach to sonicating multiple locations is shown in (a) where each location is sonicated at a repetition frequency of 1 Hz after an initial injection (i) of microbubbles, and then the same process is repeated for each point (leaving approximately 5 min in between to enable the bubbles to clear the system). The modified approach in (b) uses the capability of the positioning system to translate to six locations per second to interleave the exposures such that each location still gets sonicated at a repetition frequency of 1 Hz. This approach can result in a significant reduction in time, as well as avoids multiple injections into small animals such as mice.

cally focused with a diameter of 7 cm and a focal length of 5.6 cm. The transducer efficiency was measured to be 80%. This exposure regime is similar to previous studies aimed at achieving local opening of the blood-brain barrier in mice.[14] The individual exposures were performed separately with a fresh injection of microbubbles prior to each sonication, with a 5 min delay in between exposures to allow the ultrasound contrast agent to clear from the body. The location of BBB opening was measured with contrast-enhanced MR imaging using a T_1-weighted sequence (FSE-XL, TE=10 ms, TR =500 ms, ETL=4, 256×256, FOV=6 cm, slice=1 mm) after injection of an MR contrast agent (0.2 ml/kg, Omniscan, GE Healthcare, USA) to evaluate the spatial accuracy of the sonications. The location of enhancement was defined as the pixel with the maximum change in signal in the enhancing ROIs.

All animals were anesthetized in these acute experiments using a mixture of ketamine (0.1 mg/10 g bodyweight) and xylazine (0.07 mg/10 g bodyweight) injected intraperitoneally. Further injections (typically one-half the initial dose) were administered intraperitoneally every hour as required during the experiment depending on the duration. For all exposures the hair on the skull that lay in the path over the ultrasound beam was removed by shaving and depilation. The mice were positioned supine on the focused ultrasound exposure system with their skull positioned over the opening such that the brain was located at the focal depth of the beam. The head was placed at an appropriate angle to ensure the skull bone was transverse to the ultrasound beam to minimize beam refraction (Fig. 2). Target locations were selected from coronal or sagittal T_2-weighted MR images (FSE-XL, TE=70 ms, TR=2000 ms, ETL=4, FOV=6 cm, 128 ×128, slice=1 mm).

II.F. Multiple spot sonications

One of the features of the prototype system that can be used to increase the throughput of treatments is the capability to cover multiple spots very quickly. This enables larger regions of the brain to be exposed after a single injection of microbubbles without sacrificing the desired pulse repetition frequency for a given point. Recent results suggest that BBB opening can be achieved with a delay of up to 2 s between successive bursts of ultrasound, as measured with contrast-enhanced MR imaging.[9] In most experiments, only one location is sonicated at a time, and the system simply waits between bursts. The prototype system described in this paper is capable of translating to multiple positions in between sonications to deliver bursts to a series of targets before returning to the original location within 2 s. Given the speed of the positioning system, up to 12 separate locations (1–2 mm apart) could be exposed every 2 s which is sufficient to cover almost the entire brain in a small rodent such as the mouse. This interleaved approach reduces the experimental time to expose a specific number of locations in the brain by a factor of the number of locations and is illustrated in Fig. 3.

The capability to disrupt the BBB in multiple locations after a single bolus injection with this interleaved approach was evaluated in a rat model. Six rats (Wistar, 300–500 g) were used for this experiment, and the general experimental method with respect to anesthetic, positioning, and imaging was similar to those described above in the mice. In these experiments, however, a linear raster scan of four exposures (spaced 1.5 mm apart) was delivered to the right hemisphere of the brain after a single bolus injection of microbubbles. The exposures were delivered in 10 ms bursts at 0.558 MHz, and the total exposure time was 5 min. A spherically focused transducer with a 10 cm diameter and 8 cm focal length was used. The efficiency was measured to be 80% for this transducer. The system moved rapidly to all four points, ensuring that each location was exposed to ultrasound at a repetition frequency of 1 Hz. The capability to achieve BBB opening with this exposure was evaluated using contrast-enhanced T_1-weighted MR images, as described above.

II.G. MRI-controlled scanned ultrasound heating

Another feature of this positioning system is the capability to move a transducer during MR imaging without any mutual interference between the scanner and the system. This opens up the possibility for many types of experiments including scanned ultrasound heating with continuous MR temperature monitoring and feedback for the delivery of precise spatial heating patterns in tissue. The capability of the positioning system to perform scanned heating experiments during MR imaging was evaluated in a series of experiments in excised turkey breast. The tissue was placed over the acoustic window in the path of the acoustic beam, and scanned heating was performed using a spherically focused transducer (2.787 MHz, 5 cm diameter, 10 cm focal length). The scan path of the transducer was chosen to be circular in the *xy* plane, with radii between 2.5 and 10 mm. The period of rotation was chosen to be 1 s, and 10 W of acoustic power was delivered continuously to the tissue sample during 60 s of motion. A coronal temperature map was acquired in the plane of the focal spot to measure the spatial heating pattern produced by the scanned transducer. Temperature maps were acquired with the proton resonant frequency (PRF) shift method using a gradient echo sequence with the following parameters: (FSPGR, TE=10 ms, TR=38.6 ms, 128×128, slice=3 mm, FOV=10 cm, FA=30°), with a temporal resolution of 5 s. Temperature maps were acquired with the positioner stationary, scanning without power delivery, and scanning with power delivery to quantify the contribution of the system itself to any systematic errors in the temperature measurements due to the sensitivity of the PRF method to changes in magnetic fields.

III. RESULTS

The bench top characterization of the positioning system revealed a spatial accuracy of 0.01 mm for the stage in all three axes, measured using a dial indicator with sufficient resolution. Linear speeds up to 1 mm/s were achieved vertically, with a maximum speed of 10 mm/s in the horizontal axes. The tests in the MRI demonstrated the ability to move to desired positions while located in the bore of the 3.0 T imager with no mutual interference observed between the two systems. The activation of the motors in the MR imager ensured that no unwanted translation of the linear stages occurred during MR imaging, and no reduction in the SNR of images were observed.

Figure 4 shows the capability of the system to target multiple regions in the gel phantom in three dimensions with high accuracy. The regions of localized heating, depicted by the loss of signal intensity, coincided closely with the target position in all images. The top left image of Fig. 4 exhibits an anomalous increase in signal intensity, which could have been due to liquefaction of the gel due to excessive heating, resulting in a differential change of T_1. The target and delivered locations, as well as the distance between these points, are given in Table I, with an average spatial positioning error of 0.29 ± 0.08 mm from the target position.

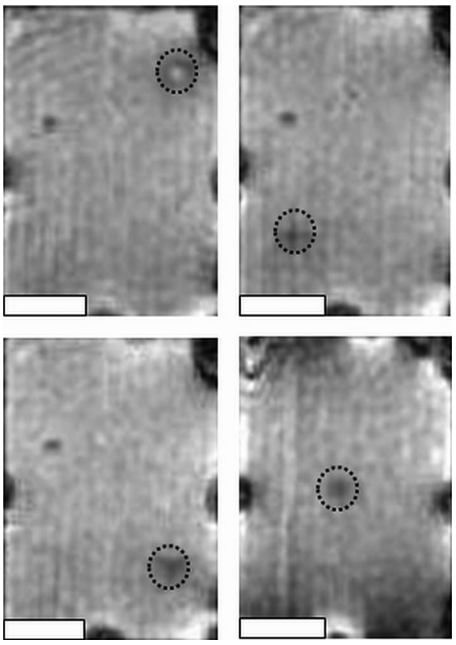

FIG. 4. Sonications in four separate locations in a gel phantom. The target location is shown by the dashed circle in each panel, and the actual focal spot location is depicted as a region of altered signal intensity within the circle due to local heating in the gel phantom. All images are transverse to the ultrasound beam direction. The white scale bar represents 10 mm.

Figure 5 shows postsonication T_1-weighted contrast-enhanced MR images of the brains of the mice exposed to focused ultrasound in two locations of the brain. The localized increase in signal intensity in the two sonicated regions depicts successful BBB opening in all of the animals. In addition, the consistency of the placement of the sonications is evident from the images. The desired separation between the two exposures was 4 mm, and the average measured separation was 3.8 ± 0.4 mm.

Figure 6 shows the results of the interleaved multiple spot exposure in a rat brain. The coronal and saggital T_1-weighted contrast-enhanced images obtained after ultrasound exposure depicts four localized regions of signal enhancement corresponding to the target locations within the brain. The variation in the spacing is likely due to variation in the skull thickness and angle causing slight shifts in the position of the acoustic focal volume at each location.

The results of the scanned heating experiments are shown in Fig. 7. During a circular scan (no ultrasound power delivery) with a 2.5 mm radius and period of 1 s [trajectory shown by the dashed circle in Fig. 7(b)], the mean temperature in a 5×5 mm^2 ROI centered about the scan trajectory varied between -0.3 and 1.2 °C. Without scanning, ROI temperature measurements fluctuated between -0.7 and 0.2 °C over the same length of time. The maximum temperature distributions (top) show that these fluctuations vary spatially but remained on the same order as the measurement uncertainty of the static case. During scanned heating [Fig. 7(c)], a large and continuous circular heating pattern was produced in the tissue sample, and the rise and fall of heating in the 5×5 ROI are clearly visualized.

TABLE I. Target ultrasound exposure locations in a gel phantom (in MR imaging coordinates) and the corresponding locations measured with MR thermometry (delivered). The mean absolute distance between the delivered and planned locations was 0.3 mm. The increase in error compared with the bench top measurements was attributed to the initial calibration of the focal spot location prior to the measurements.

	Target						Delivered						$\|R\|$
Location	L/R		A/P		S/I		L/R		A/P		S/I		(mm)
1	6.3	L	13.4	A	16	S	6.2	L	13.6	A	15.8	S	0.35
2	7.7	R	13.4	A	3.4	I	7.9	R	13.6	A	3.6	I	0.39
3	6.3	L	13.4	A	4.1	I	6.2	L	13.6	A	4.4	I	0.35
4	1.7	R	17.4	A	5.2	S	1.8	R	17.3	A	5.2	S	0.16
5	0.7	R	9.4	A	13.5	S	0.7	R	9.4	A	13.2	S	0.26
6	0.7	R	9.4	A	3.7	I	0.8	R	9.4	A	3.9	I	0.26
Average													$0.29 \pm .08$

IV. DISCUSSION

An MRI-compatible focused ultrasound system designed for use with small animal models has been developed and characterized. The system is capable of positioning an ultrasound focal volume in three dimensions with a spatial accuracy of about 0.3 mm and can be used to deliver multiple spots along a desired trajectory. The excellent MRI compatibility of the system enables simultaneous imaging and motion with the system without mutual interference. These features were obtained through the use of custom non-magnetic linear stages driven by piezoceramic motors and optical encoders. Both the motors and encoders are driven by sinusoidal signals at frequencies much lower than the bandwidth of the MR imager (~40–100 kHz) enabling good isolation between the two systems. The range of motion of the system (5 cm horizontal, 2.5 cm vertical) is sufficient for small animal studies but could easily be extended to over 20 cm in the horizontal directions with the current stage design if desired.

The interleaved approach shown in Fig. 6 to open the BBB in multiple locations in the rat brain from a single contrast agent injection is an attractive feature of this technology. This approach has three main benefits. The first is the reduction in time for a single experiment in an animal by up to as much as a factor of 6. This represents very important savings in time when considering experiments in the MR imaging environment. The second benefit is the generation of a desired bioeffect at the same time in multiple locations, which enables the use of a single contrast-enhanced MR image to evaluate the overall extent of BBB opening in the brain. This is important since the MR contrast agents can have some level of toxicity in the brain, which could be compounded with multiple injections. In addition, the time dependence of the extent of BBB opening makes quantitative analysis of the signal intensity on contrast-enhanced MR images difficult if the sonications were delivered at different times. The final benefit of this approach is the capability to perform the entire experiment with only a single injection of ultrasound and MR contrast agents. This reduces the volume of fluids injected into the animal, which is very important in smaller and more sensitive species such as mice. The interleaved sonication strategy can also be extended to other applications requiring intermittent pulses of ultrasound in locations other than the brain.[30,31] Beyond BBB disruption, this system has applications in a range of therapeutic ultrasound experiments. In particular, the system can be used to deliver continuous exposures of ultrasound precisely to soft tissue targets for heating and other bioeffects in raster, scanned, or other spatial patterns. The capability to perform simultaneous MR imaging and motion enables on-line temperature measurements of the spatial heating pattern during energy deliv-

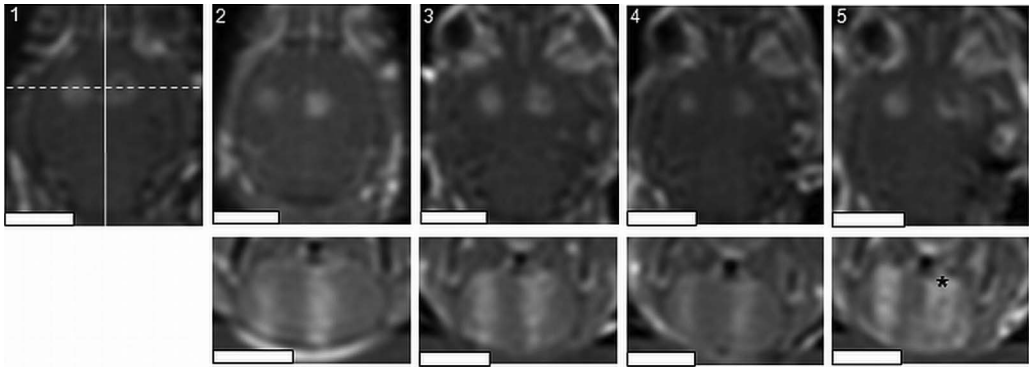

FIG. 5. Multiple exposures in a mouse model, repeated successively in five animals. Repeatable opening of the blood-brain barrier is achieved with consistent focal spot placement in the brains of all the animals. The reduced signal intensity in the lower-right sonication (*) may be indicative of tissue damage. The spacing between the exposures is approximately 4 mm. The bottom panels are perpendicular to the top panels along the dotted line in 1, and the scale bars represent 5 mm. The width of the images is approximately 1.4 cm.

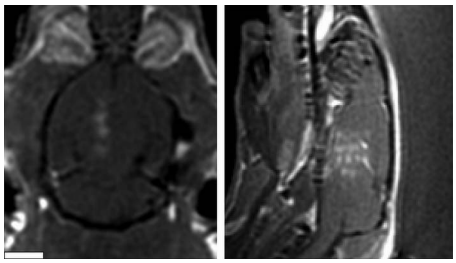

FIG. 6. Example of a scanned linear exposure in a rat brain aimed at opening the BBB in a larger volume of the brain. Four exposures separated by 1.5 mm were delivered in a linear scan, approximately 0.25 s apart, resulting in an individual repetition frequency of 1 Hz for each spot. The overall exposure lasted 5 min. The white scale bar represents 5 mm. The coronal (left) and saggital (right) contrast-enhanced images show the region of signal enhancement corresponding to local opening of the BBB.

ery. The heating experiments in Fig. 7 demonstrate the feasibility of accurate temperature imaging using the PRF technique during circular scanning, enabling this system to continuously heat volumes greater than the focal volume under MR temperature feedback control. These trajectories are easily selected and modified, allowing greater flexibility and reduced complexity than phased array systems for customizing target regions during small animal experiments.

A similar exposure pattern could be delivered with phased array transducer systems; however, this would require complex electronics to achieve the appropriate phase delays. The switching speed of a phased array design would be faster than the motor system which is limited by the maximum velocity of the motors to delivering up to six spots per second with the current design. The level of repeatability and speed achieved with this system is still sufficient to enable high-throughput investigation of drug delivery to the brain using focused ultrasound in small animal models. We envision this platform as being suitable for investigating novel delivery strategies and approaches to inform the subsequent design of more customized phased array systems for advanced preclinical or clinical use.

The degradation in the accuracy of spatial positioning in the MRI as compared with the bench top tests was most likely due to errors in calibration of the transducer focal position in MR imaging coordinates at the beginning of the experiment using the method described above. In addition some of the uncertainty in positioning in the brain studies is due to the potential refraction of the ultrasound beam as it passes through the skull bone. Nonetheless, the accuracy of ultrasound delivery in these experiments was on the order of the pixel dimensions in the MR images, which is acceptable.

Overall, the MRI-compatible positioning system described in this manuscript is well adapted in performing high-throughput focused ultrasound experiments in small animal models for the development of drug delivery strate-

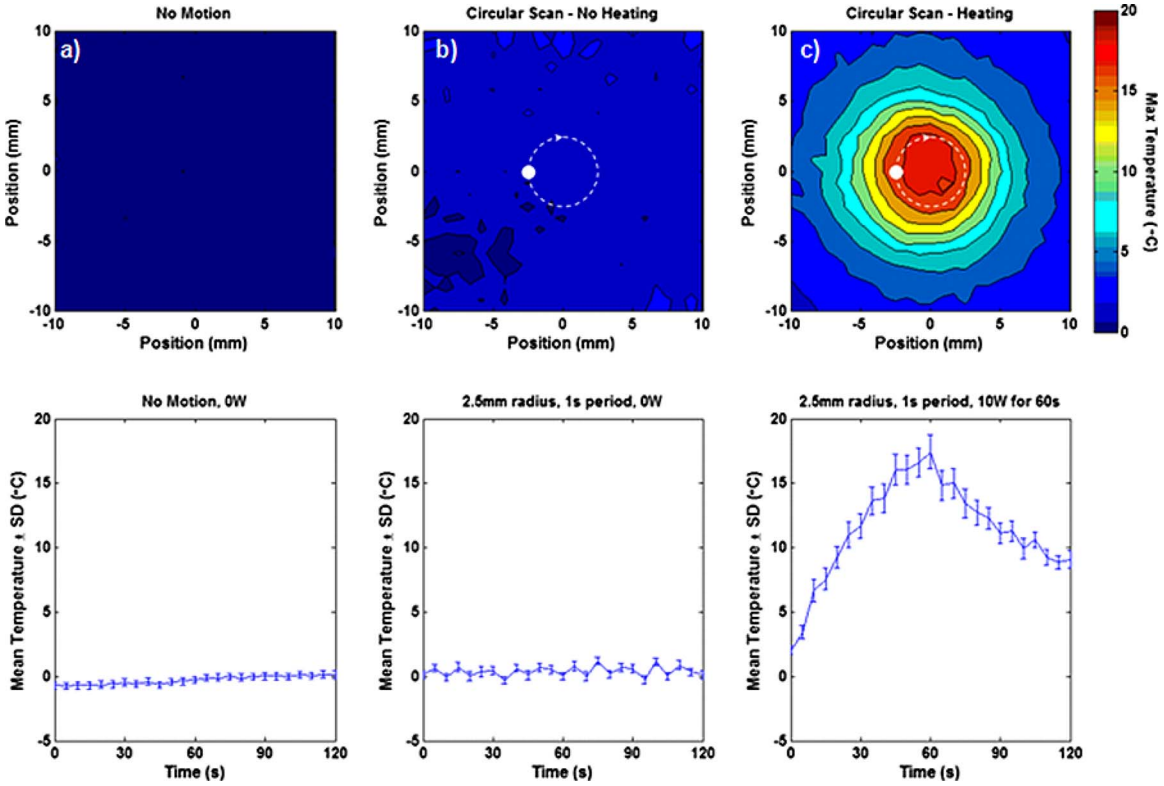

FIG. 7. Example of using the positioning system to perform scanned ultrasound heating with simultaneous MR thermometry. The top row shows the maximum temperature distribution measured in excised turkey breast with (a) the positioner stationary, (b) moving in a circular path with a 2.5 mm radius and a period of 1 s, and (c) moving in the same circular path with 10 W of acoustic energy delivered for 60 s in order to produce a large heating pattern. No ultrasound energy was delivered in (a) or (b). The bottom row shows the mean temperature of a 5×5 mm^2 ROI that depicts the minimal impact presented by the motion of the positioning system on the MR thermometry measurements.

gies in the brain and other organs. Rapid exposure of large regions in the brain can be achieved in short times using an interleaved approach, with the ability to target specific anatomical regions within the body.

ACKNOWLEDGMENTS

This work was supported by the National Institutes of Health (Grant No. R01EB003268 and R33EB000705), Canada Research Chair Program, and the Ontario Research Commercialization Program from the Ministry of Research and Innovation. The authors wish to thank Ms. Shawna Rideout for her assistance with the experiments described in this study in the rats and mice.

[a]Electronic mail: chopra@sri.utoronto.ca

[1]K. Hynynen *et al.*, "MR imaging-guided focused ultrasound surgery of fibroadenomas in the breast: A feasibility study," Radiology **219**, 176–185 (2001).
[2]F. M. Fennessy and C. M. Tempany, "MRI-guided focused ultrasound surgery of uterine leiomyomas," Acad. Radiol. **12**, 1158–1166 (2005).
[3]C. M. Tempany *et al.*, "MR imaging-guided focused ultrasound surgery of uterine leiomyomas: A feasibility study," Radiology **226**, 897–905 (2003).
[4]R. Deckers, C. Rome, and C. T. Moonen, "The role of ultrasound and magnetic resonance in local drug delivery," J. Magn. Reson. Imaging **27**, 400–409 (2008).
[5]M. Kinoshita *et al.*, "Targeted delivery of antibodies through the blood-brain barrier by MRI-guided focused ultrasound," Biochem. Biophys. Res. Commun. **340**, 1085–1090 (2006).
[6]K. Hynynen, "Focused ultrasound for blood-brain disruption and delivery of therapeutic molecules into the brain," Expert Opin. Drug Deliv. **4**, 27–35 (2007).
[7]M. Kinoshita *et al.*, "Targeted delivery of antibodies through the blood-brain barrier by MRI-guided focused ultrasound," Biochem. Biophys. Res. Commun. **340**, 1085–1090 (2006).
[8]D. P. Madio *et al.*, "On the feasibility of MRI-guided focused ultrasound for local induction of gene expression," J. Magn. Reson. Imaging **8**, 101–104 (1998).
[9]N. McDannold, N. Vykhodtseva, and K. Hynynen, "Effects of acoustic parameters and ultrasound contrast agent dose on focused-ultrasound induced blood-brain barrier disruption," Ultrasound Med. Biol. **34**, 930–937 (2008).
[10]N. McDannold, N. Vykhodtseva, and K. Hynynen, "Use of ultrasound pulses combined with definity for targeted blood-brain barrier disruption: A feasibility study," Ultrasound Med. Biol. **33**, 584–590 (2007).
[11]K. Hynynen *et al.*, "Noninvasive MR imaging-guided focal opening of the blood-brain barrier in rabbits," Radiology **220**, 640–646 (2001).
[12]K. Hynynen *et al.*, "The threshold for brain damage in rabbits induced by bursts of ultrasound in the presence of an ultrasound contrast agent (optison)," Ultrasound Med. Biol. **29**, 473–481 (2003).
[13]J. J. Choi *et al.*, "Spatio-temporal analysis of molecular delivery through the blood-brain barrier using focused ultrasound," Phys. Med. Biol. **52**, 5509–5530 (2007).
[14]M. Kinoshita *et al.*, "Noninvasive localized delivery of herceptin to the mouse brain by MRI-guided focused ultrasound-induced blood-brain barrier disruption," Proc. Natl. Acad. Sci. U.S.A. **103**, 11719–11723 (2006).
[15]L. H. Treat *et al.*, "Targeted delivery of doxorubicin to the rat brain at therapeutic levels using MRI-guided focused ultrasound," Int. J. Cancer **121**, 901–907 (2007).
[16]K. Chinzei and K. Miller, "Towards MRI guided surgical manipulator," Med. Sci. Monit. **7**, 153–163 (2001).
[17]E. Hempel *et al.*, "An MRI-compatible surgical robot for precise radiological interventions," Comput. Aided Surg. **8**, 180–191 (2003).
[18]N. V. Tsekos, A. Ozcan, and E. Christoforou, "A prototype manipulator for magnetic resonance-guided interventions inside standard cylindrical magnetic resonance imaging scanners," J. Biomech. Eng. **127**, 972–980 (2005).
[19]B. T. Larson *et al.*, "Design of an MRI-compatible robotic stereotactic device for minimally invasive interventions in the breast," J. Biomech. Eng. **126**, 458–465 (2004).
[20]A. Krieger *et al.*, "Design of a novel MRI compatible manipulator for image guided prostate interventions," IEEE Trans. Biomed. Eng. **52**, 306–313 (2005).
[21]M. Muntener *et al.*, "Magnetic resonance imaging compatible robotic system for fully automated brachytherapy seed placement," Urology **68**, 1313–1317 (2006).
[22]R. Salomir *et al.*, "Local hyperthermia with MR-guided focused ultrasound: Spiral trajectory of the focal point optimized for temperature uniformity in the target region," J. Magn. Reson. Imaging **12**, 571–583 (2000).
[23]D. Arora *et al.*, "Control of thermal therapies with moving power deposition field," Phys. Med. Biol. **51**, 1201–1219 (2006).
[24]H. E. Cline *et al.*, "Focused US system for MR imaging-guided tumor ablation," Radiology **194**, 731–737 (1995).
[25]K. Hynynen *et al.*, "MRI-guided noninvasive ultrasound surgery," Med. Phys. **20**, 107–115 (1993).
[26]P. E. Huber *et al.*, "A new noninvasive approach in breast cancer therapy using magnetic resonance imaging-guided focused ultrasound surgery," Cancer Res. **61**, 8441–8447 (2001).
[27]L. Curiel, R. Chopra, and K. Hynynen, "Progress in multimodality imaging: Truly simultaneous ultrasound and magnetic resonance imaging," IEEE Trans. Med. Imaging **26**, 1740–1746 (2007).
[28]K. Hynynen *et al.*, "Noninvasive MR imaging-guided focal opening of the blood-brain barrier in rabbits," Radiology **220**, 640–646 (2001).
[29]N. McDannold *et al.*, "MRI-guided targeted blood-brain barrier disruption with focused ultrasound: Histological findings in rabbits," Ultrasound Med. Biol. **31**, 1527–1537 (2005).
[30]V. Frenkel, "Ultrasound mediated delivery of drugs and genes to solid tumors," Adv. Drug Delivery Rev. **60**, 1193–1208 (2008).
[31]B. E. O'Neill *et al.*, "Pulsed high intensity focused ultrasound mediated nanoparticle delivery: Mechanisms and efficacy in murine muscle," Ultrasound Med. Biol. **35**, 416–424 (2009).